



Article

An Assessment of the Lancaster Sound Polynya Using Satellite Data 1979 to 2022

R.F. Vincent

Department of Physics and Space Science, Royal Military College of Canada, Kingston, ON K7K 7B4, Canada; ron.vincent@rmc.ca

Abstract: Situated between Devon Island and Baffin Island, Lancaster Sound is part of *Tallurutiup Imanga*, which is in the process of becoming the largest marine conservation area in Canada. The cultural and ecological significance of the region is due, in part, to a recurring polynya in Lancaster Sound. The polynya is demarcated by an ice arch that generally forms in mid-winter and collapses in late spring or early summer. Advanced Very High Resolution imagery from 1979 to 2022 was analyzed to determine the position, formation and collapse of the Lancaster Sound ice arch. The location of the ice arch demonstrates high interannual variability, with 512 km between the eastern and western extremes, resulting in a polynya area that can fluctuate between 6000 km² and 40,000 km². The timing of the seasonal ice arch formation and collapse has implications with respect to ice transport through Lancaster Sound and the navigability of the Northwest Passage. The date of both the formation and collapse of the ice arch is variable from season to season, with the formation observed between November and April and collapse usually occurring in June or July. A linear trend from 1979 to 2022 indicates that seasonal ice arch duration has declined from 150 to 102 days. The reduction in ice arch duration is a result of earlier collapse dates over the study period and later formation dates, particularly from 1979 to 2000. Lancaster Sound normally freezes west to east each season until the ice arch is established, but there is no statistical relationship between the ice arch location and duration. Satellite surface temperature mapping of the region indicates that the polynya is characterized by sub-resolution leads during winter.

Keywords: remote sensing; arctic waters; Lancaster Sound; polynya; ice arch; sea ice; AVHRR; sea surface temperature; ice surface temperature



Citation: Vincent, R.F. An Assessment of the Lancaster Sound Polynya Using Satellite Data 1979 to 2022. *Remote Sens.* **2023**, *15*, 954. <https://doi.org/10.3390/rs15040954>

Academic Editors: Tonghua Wu, Florent Garnier, Lin Liu and Yubao Qiu

Received: 30 December 2022
Revised: 31 January 2023
Accepted: 6 February 2023
Published: 9 February 2023



Copyright: © 2023 by the author. Licensee MDPI, Basel, Switzerland. This article is an open access article distributed under the terms and conditions of the Creative Commons Attribution (CC BY) license (<https://creativecommons.org/licenses/by/4.0/>).

1. Introduction

Polynyas are regions in the polar maritime environment that remain relatively ice-free under conditions that should dictate thick ice cover. There are several mechanisms of polynya maintenance that are not necessarily mutually exclusive [1]. Open water may be maintained through latent heat of fusion from the continuous formation of new ice as floes are swept away by wind and currents [2]. Another mechanism of polynya maintenance is the introduction of sensible heat from depth due to upwelling induced by wind or currents [3,4]. Additionally, the breaking up of ice may occur in regions that experience large tidal amplitudes [5–7]. During the winter months, polynyas create an ocean-to-atmosphere heat flux about two orders of magnitude higher than the surrounding pack ice [8]. These oceanographic oases are zones of significant biodiversity and productivity, forming important habitats for marine mammals and birds [9–11]. There are more than twenty recurring polynyas in the Canadian Arctic, including one in Lancaster Sound [7].

Situated between Devon Island and Baffin Island, Lancaster Sound represents the eastern entrance to the Northwest Passage (Figure 1). It extends 300 km east of Bylot Island and becomes Barrow Strait at the eastern edge of Somerset Island. The Lancaster Sound/Barrow Strait system is 550 km in length, with an average width of approximately 75 km. The surface currents flow westward along the northern part of the sound and eastward on the southern portion [12]. The tides in the region are significant, with a maximum amplitude of

approximately 3 m at Dundas Harbor and lessening westward to about 2 m at Resolute [13]. Acoustic Doppler current profiler observations show that the currents in Lancaster Sound are dominated by tides in the two along-strait directions [14]. The water depth becomes shallower from east to west, ranging from 800 m at Bylot Island to 200 m in Barrow Strait [15–17]. Lancaster Sound is in the region known as *Tallurutiup Imanga*, which is in the process of becoming the largest marine conservation area in Canada because of its cultural and ecological significance [16,18]. A major reason for the abundance and biodiversity of marine life in Lancaster Sound is the annual formation of a polynya during the colder months.

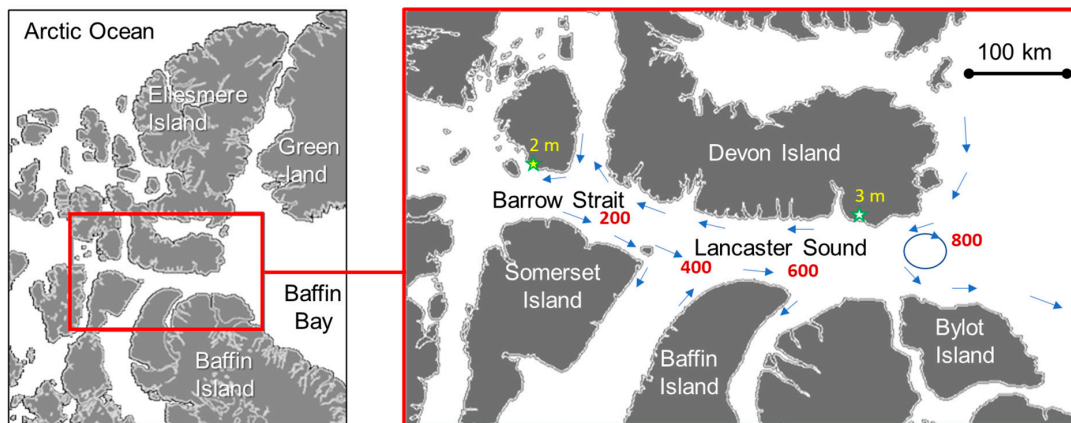


Figure 1. Location of Lancaster Sound and Barrow Strait. Surface current direction is shown by the blue arrows, while depth in meters is indicated in red. Maximum tidal amplitudes at Dundas Harbor (3 m) and Resolute (2 m) are depicted with stars.

The western extent of the Lancaster Sound polynya is demarcated by an ice arch that generally forms in mid-winter and collapses in late spring or early summer. Ice arches are common features in the narrow water passages of the Canadian Archipelago, creating distinct borders between the frozen pack ice and relatively ice-free regions [19]. Polynyas in the eastern Canadian Arctic, including the North Water (NOW), Jones Sound, Hell Gate and Dundas Island, feature ice arches that form seasonally in the same general location; however, the position of the Lancaster Sound ice arch fluctuates dramatically and may occur anywhere in Lancaster Sound or further west in Barrow Strait (Figure 2). The distance between the eastern- and western-most ice arch location is more than 500 km, resulting in a polynya area that can fluctuate interannually between 6000 km² and 40,000 km². The timing of the seasonal ice arch formation and collapse has implications with respect to ice transport through Lancaster Sound and the navigability of the Northwest Passage.

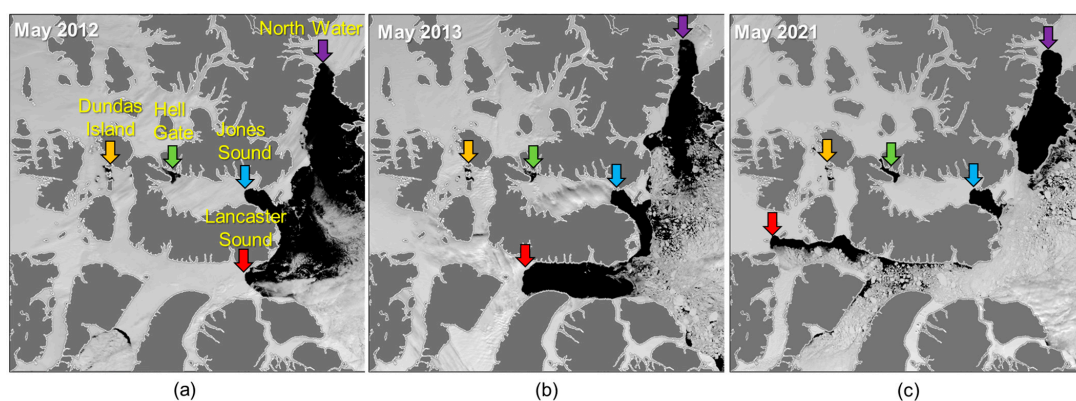


Figure 2. Satellite images with land mask showing the location of five recurring polynyas (North Water, Dundas Island, Hell Gate, Jones Sound and Lancaster Sound) in the eastern Arctic for (a) May

2012, (b) May 2013 and (c) May 2021. Ice arch location for each polynya is shown with a color-coded arrow. The location of the Lancaster Sound ice arch can vary by more than 500 km, even extending into Barrow Strait, significantly changing the area of the polynya.

This research analyzes the formation and collapse of the Lancaster Sound ice arch using satellite imagery from 1979 to 2022. Following a description of methods used in the study, the location and timing of ice arch consolidation and subsequent collapse is examined for each year. The trends and implications of the results are discussed, followed by conclusions.

2. Materials and Methods

Satellite remote sensing of Arctic waters is well-established using an array of tools including synthetic aperture radar, multispectral sensors, passive microwave and radar altimetry [20–23]. While all of these techniques have inherent strengths, Advanced Very High Resolution Radiometry (AVHRR) imagery was chosen for this research because of its ease of processing, extensive Arctic coverage and long heritage. Launched in October 1978, TIROS-N was the first satellite to carry an AVHRR. This was followed by the National Oceanic and Atmospheric Administration (NOAA) series from NOAA-6 to NOAA-19, and the European Space Agency MetOp satellites (A, B and C). There has been continuous coverage of the Earth by AVHRR since the launch of TIROS-N (Table 1). The AVHRR sensor uses a combination of visible, near/middle infrared and thermal infrared (TIR) channels (Table 2). AVHRR-equipped satellites are in polar low Earth orbits that image the Arctic 14 to 15 times per day with a swath width of about 3000 km. The study area was imaged approximately seven times per day, with a temporal resolution of approximately 100 min between successive passes. Spatial resolution at nadir is 1.1 km for all channels, which degrades to about 8 km toward the edge of the swath. File formats offering the best spatial resolution are High Resolution Picture Transmission (HRPT) for NOAA satellites and Full Resolution Area Coverage (FRAC) for MetOp satellites. Global Area Coverage (GAC) format for NOAA satellites with a nadir resolution of 4 km was used for earlier images when appropriate HRPT data were not available in the database. Generally, GAC data were used 1979 to 1998, while HRPT and FRAC imagery were available 1999 to 2022. The spatial resolution of GAC images proved adequate for analyzing ice arch structures in Lancaster Sound. AVHRR data for this study were retrieved online from NOAA’s Comprehensive Large Array-data Stewardship System [24].

Table 1. Satellites equipped with the AVHRR sensor. The most recent NOAA polar orbiting satellites, NOAA-20 (launched 2017) and NOAA-21 (launched 2022), replaced the AVHRR with the Visible Infrared Imaging Radiometer Suite developed from the Moderate Resolution Imaging Spectroradiometer flown on the Aqua and Terra satellites.

Satellite	Years Active	Satellite	Years Active
TIROS-N	1978–1981	NOAA-14	1994–2007
NOAA-6	1979–1981	NOAA-15	1998–Present
NOAA-7	1981–1986	NOAA-16	2000–2014
NOAA-8	1983–1985	NOAA-17	2002–2013
NOAA-9	1984–1998	NOAA-18	2005–Present
NOAA-10	1986–2001	MetOp-A	2006–2021
NOAA-11	1988–2004	NOAA-19	2009–Present
NOAA-12	1998–2007	MetOp-B	2012–Present
NOAA-13	1993–1993	MetOp-C	2018–Present

Table 2. AVHRR specifications for NOAA and METOP satellites. Categories are AVHRR/3 (all channels), AVHRR/2 (minus Channel 3A) and AVHRR/1 (minus Channel 3A and Channel 5).

Channel	Wavelength (um)	Description	Satellites
1	0.58–0.68	Visible	All satellites
2	0.725–1.00	Visible/Near infrared	All satellites
3A	1.58–1.64	Near Infrared	NOAA-15 to -19 and MetOp series
3B	3.55–3.93	Middle Infrared	NOAA-8 to -19 and MetOp series
4	10.30–11.30	Thermal Infrared	All satellites
5	11.50–12.50	Thermal Infrared	NOAA-8 to -19 and MetOp series

The location and date of the Lancaster Sound ice arch was determined for each season from 1979 to 2022 by visual inspection of satellite imagery. In all cases, TIR was used to determine ice arch formation, while visible wavelengths proved superior for observing ice arch collapse. Ice arch formation occurred when it achieved the characteristic shape for the season, while collapse was characterized by the breakdown of the structure (Figure 3). Extensive cloud cover during the warmer months [25] was mitigated by the high number of satellite passes per day. Ice arch formation, which occurred during the colder months, was relatively straight forward because of the decreased cloud cover and excellent ice/water contrast offered by TIR imagery. The uncertainty for ice arch formation and collapse is ± 2 days.

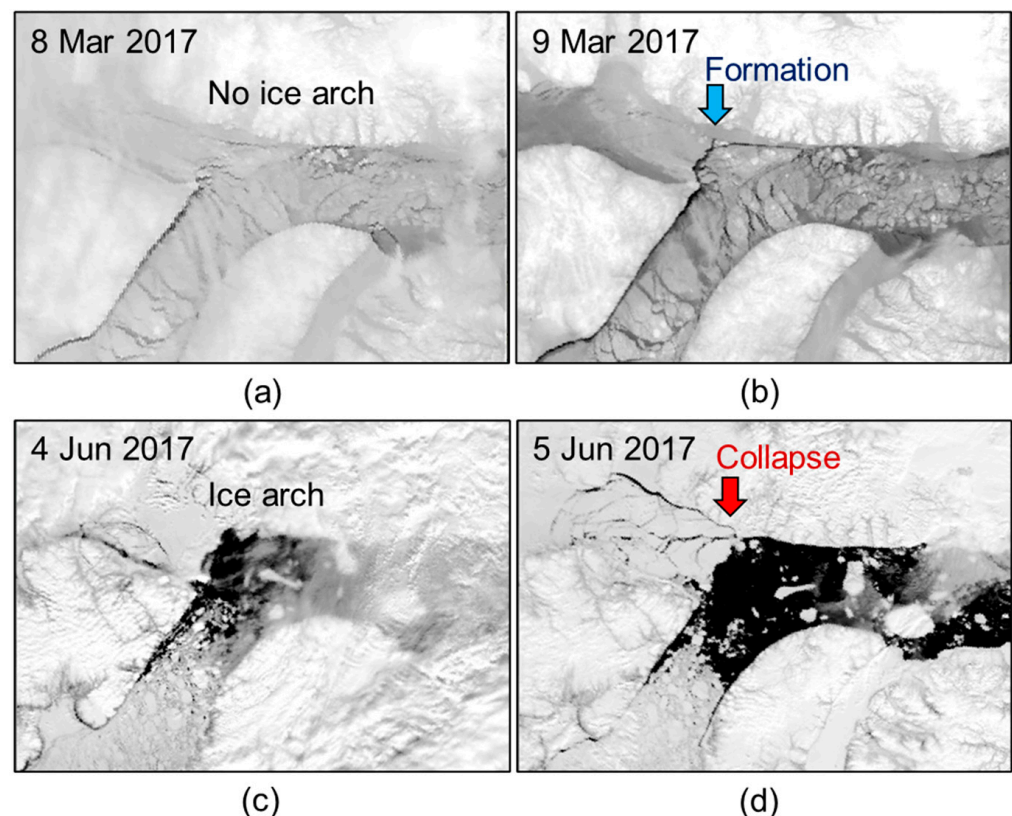


Figure 3. Example of the determination of ice arch formation (thermal infrared) and collapse (visible) in Lancaster Sound. (a) On 8 March 2017, the ice arch is not apparent. (b) The following day, the ice arch has formed. (c) The characteristic shape is maintained until 4 June 2017. (d) The ice arch collapses the following day.

Sea and ice surface temperatures were calculated using the single channel Composite Arctic Sea Surface Temperature Algorithm (CASSTA) [26]. The algorithm uses Channel 4 to determine the surface temperature of seawater, ice, and marginal ice zones. The use of a single channel aims to reduce the inaccuracies of split window algorithms in the Arctic environment [27]. The single channel CASSTA was created for the METOP-A AVHRR sensor and restricted to data collected by that satellite (2006 to 2021).

3. Results

3.1. Location of Ice Arch 1979 to 2022

The satellite imagery showed that the Barrow Strait/Lancaster Sound system generally freezes from west to east each season. Temporary ice arches sometimes formed for several days or weeks before migrating eastward to the final position (Figure 4). On two occasions (1992, 2004), the ice arch appeared consolidated and then moved westward. Ice floes were consistently observed to move eastward on consecutive satellite images, supporting latent heat of fusion as one mechanism of polynya maintenance. The terminal points of the ice arch are generally anchored to large land masses in Lancaster Sound, while beyond Somerset Island, the structure end points are contained by small islands in Barrow Strait (Figure 5).

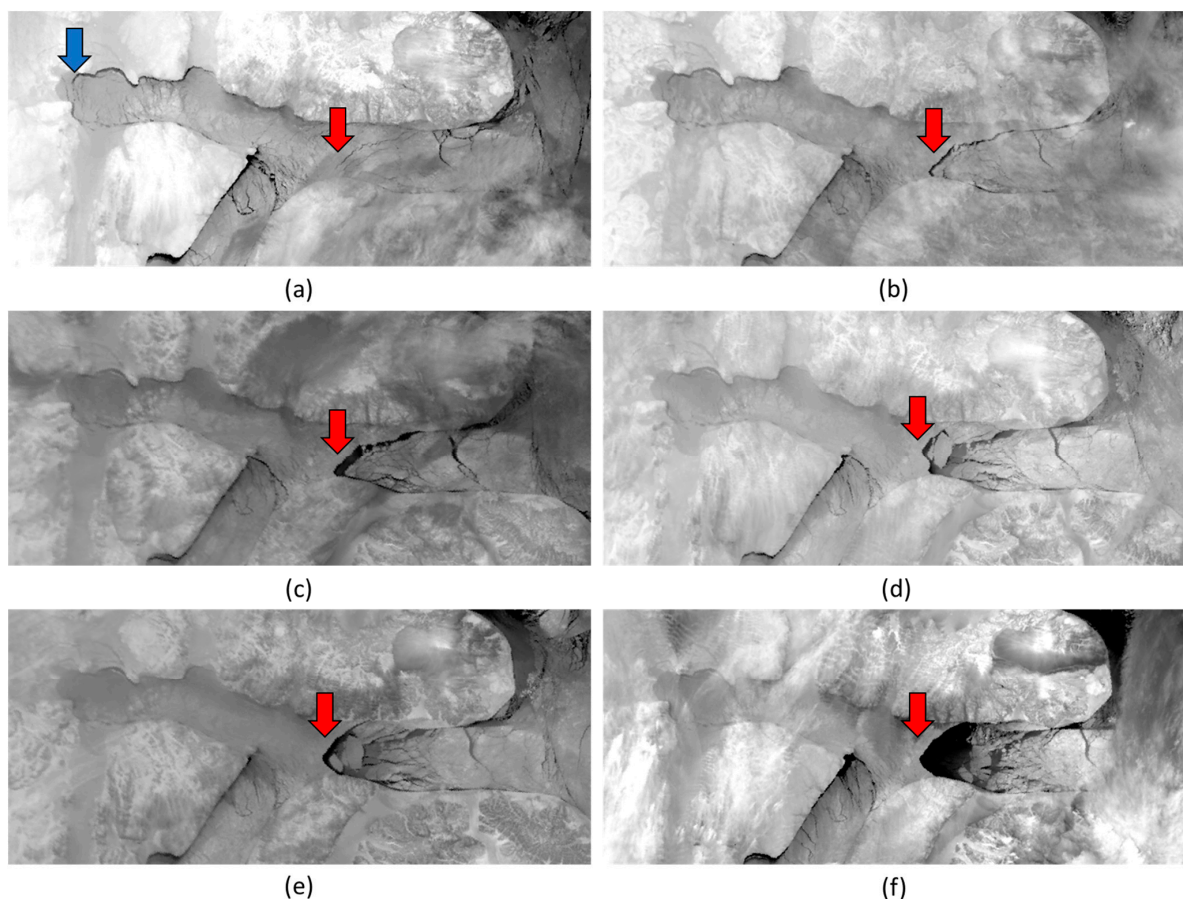


Figure 4. Sequence of satellite images showing the formation of the Lancaster Sound ice arch in 2019 for (a) 28 January, (b) 30 January, (c) 1 February, (d) 3 February, (e) 5 February and (f) 7 February. The ice arch appears established on 28 January (blue arrow), but a small break in the ice cover appears further east on the same day (red arrow). Over the next week, the new ice arch becomes established (red arrows), and remains constant until collapse on 18 June, while the ice to the west is frozen solid. This was a common sequence for the ice arch formation in Lancaster Sound. The movement of the ice is eastward from the arch.

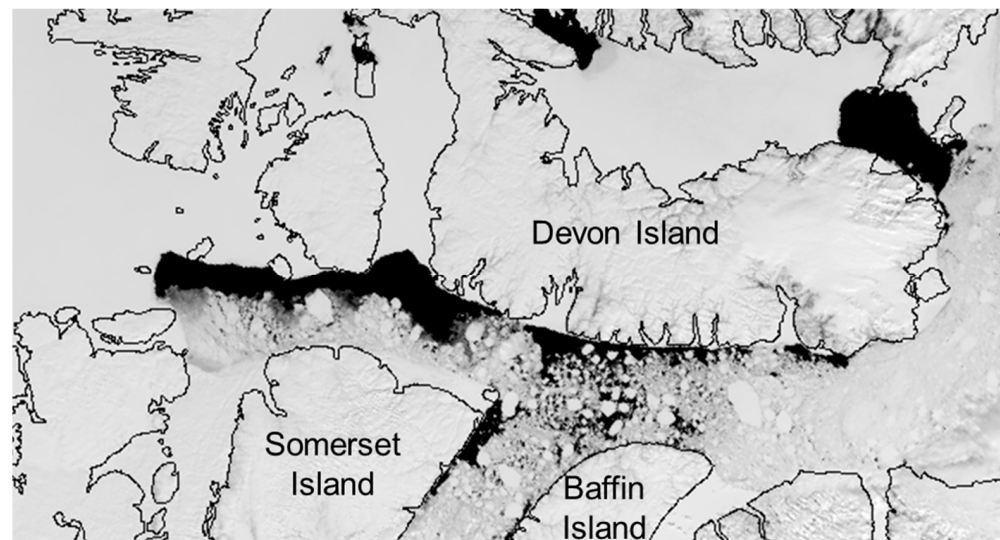


Figure 5. Satellite image with coastlines outlined of the ice arch in Barrow Strait on 24 May 2021. The terminal points on the ice arch are contained within small islands.

The distance to the ice arch for each year was measured nominally from the northwestern point of Bylot Island. For consistency, the western-most point of the ice arch was chosen for the measurement. The following are statistics for ice arch distance from Bylot Island.

- Minimum Distance: 33 km (1983);
- Maximum Distance: 545 km (1986, 2010, 2021);
- Average Distance: 273 km ($\sigma = 144$ km);
- Linear Trend 1979 to 2022: Increase 214 km to 329 km ($R^2 = 0.0548$, p -value = 0.1262).

The ice arch location from year to year is highly variable (Figure 6). The average distance between ice arches from one year to the next from 1979 to 2022 is 150 km. The high variability gives a low R^2 value, while the p -value indicates that the linear trend of ice arches occurring 115 km further to the west is not statistically significant. The minimum, average (approximate) and maximum ice arch distances are shown in Figure 2a–c, respectively. For distances beyond 300 km, the ice arch is technically in Barrow Strait, but both the structure and polynya will be referred to as Lancaster Sound in this paper.

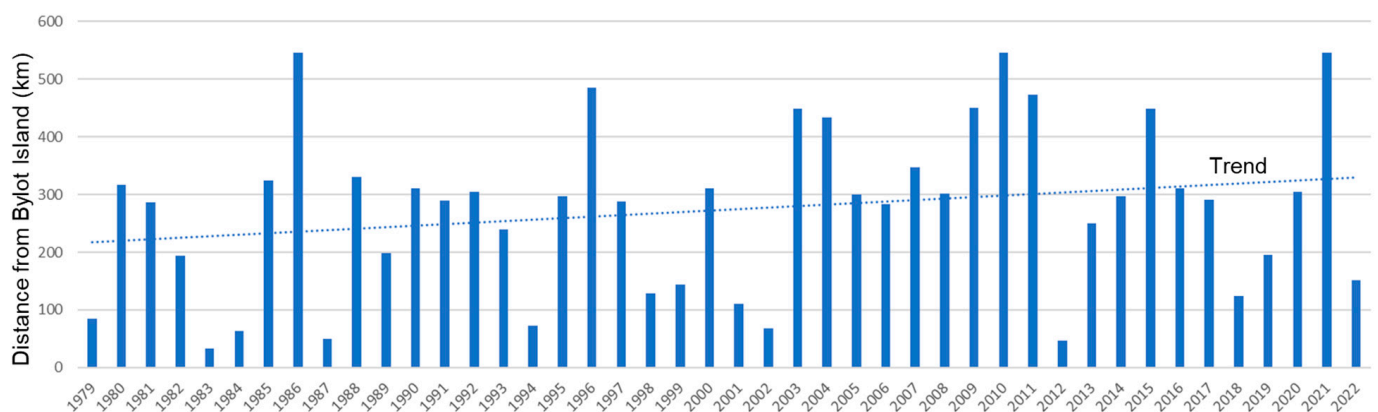


Figure 6. Distance in kilometers from Bylot Island to the Lancaster Sound ice arch for 1979 to 2022. The location of the ice arch is highly variable ($R^2 = 0.0548$) on an interannual basis, while the overall westward trend of 115 km is statistically weak (p -value = 0.1262).

3.2. Timing of Ice Arch Formation and Collapse

The Lancaster Sound ice arch generally forms between January and March. On three occasions, consolidation occurred before January, (1979, 1980, 2015 seasons, which refers to the year of ice arch collapse), while formation in April was confined to four years (1998, 1999, 2000, 2015). The following are statistics for the date of ice arch formation.

- Earliest Formation: 27 November (1979 season);
- Latest Formation: 17 April (1999);
- Average: 18 February ($\sigma = 36$ Days);
- Trend: 5 February to 3 March: Increase of 26 days ($R^2 = 0.0631$, p -value = 0.1000).

The Lancaster Sound ice arch usually collapses in late June or early July as surface air temperatures in the region rise above the freezing point. All ice arch collapses occurred in June or July except for 2010, when it happened on 29 April, which is 36 days sooner than the next earliest. The following are statistics for the date of the ice arch collapse.

- Earliest Collapse: 29 April (2010);
- Latest Collapse: 25 July (1986);
- Average: 23 June ($\sigma = 14$ Days);
- Trend: 5 July to 13 June: Decrease of 22 days ($R^2 = 0.1898$, p -value = 0.0031).

The determination of the ice arch formation and collapse (Figure 7) allows the calculation of the ice arch duration for each year (Figure 8). The ice arch generally persists for about four months. For three years, it lasted over 180 days (1979, 1980, 1987), while two years (1998, 1999) experienced ice arch duration of less than 60 days. The following are statistics for the duration of ice arch of formation.



Figure 7. Formation and collapse of the Lancaster Sound ice arch from 1979 to 2022. Formation date of the ice arch is more variable than the collapse date. Ice arch formation is trending toward later dates, while collapse of the structure is trending toward earlier dates. The formation trend is statistically weak (p -value = 0.1000), but the collapse trend is statistically significant (p -value = 0.0031).

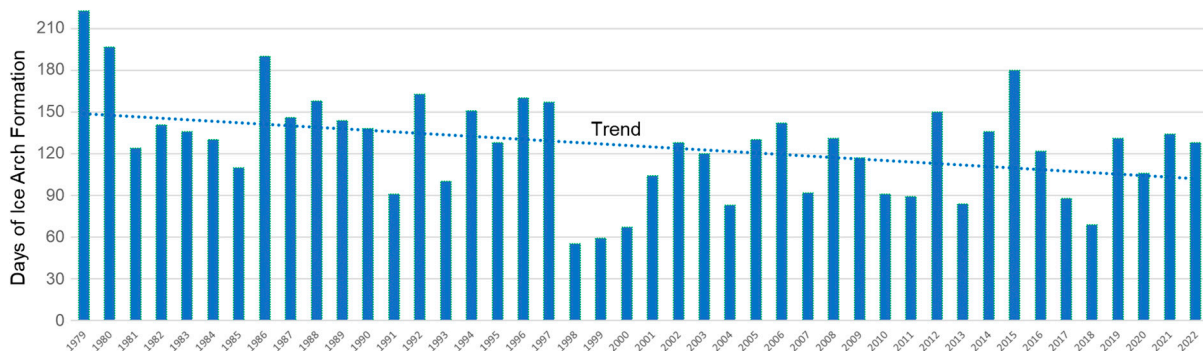


Figure 8. Duration in days of the Lancaster Sound ice arch for 1979 to 2022. Interannual variations in ice arch duration predominate the record ($R^2 = 0.1492$), but the overall trend is a reduction of 48 days, which is statistically significant (p -value = 0.0100).

- Minimum Ice Arch Duration: 55 days;
- Maximum Ice Arch Duration: 223 days;
- Average: 126 days, $\sigma = 36$ days;
- Linear Trend: Decrease 150 days to 102 days ($R^2 = 0.1492$, p -value = 0.0100).

3.3. Sea and Ice Surface Temperatures

Sea and ice surface temperatures were determined using the single channel CASSTA for MetOp-A images. Prior to ice arch consolidation, the surface temperatures in Lancaster Sound and Barrow Strait tended toward the temperature of the surrounding ice pack. In some years, it appeared that Lancaster Sound may freeze completely, but a break in the ice and eastward movement of floes from the break would lead to the ice arch formation (Figure 4). Once the ice arch formed and the polynya was established, the surface temperatures warmed east of the ice arch and provided a stark contrast to the surface temperatures west of the ice arch (Figure 9). The polynya surface temperatures remained comparatively warm until ice arch collapse.

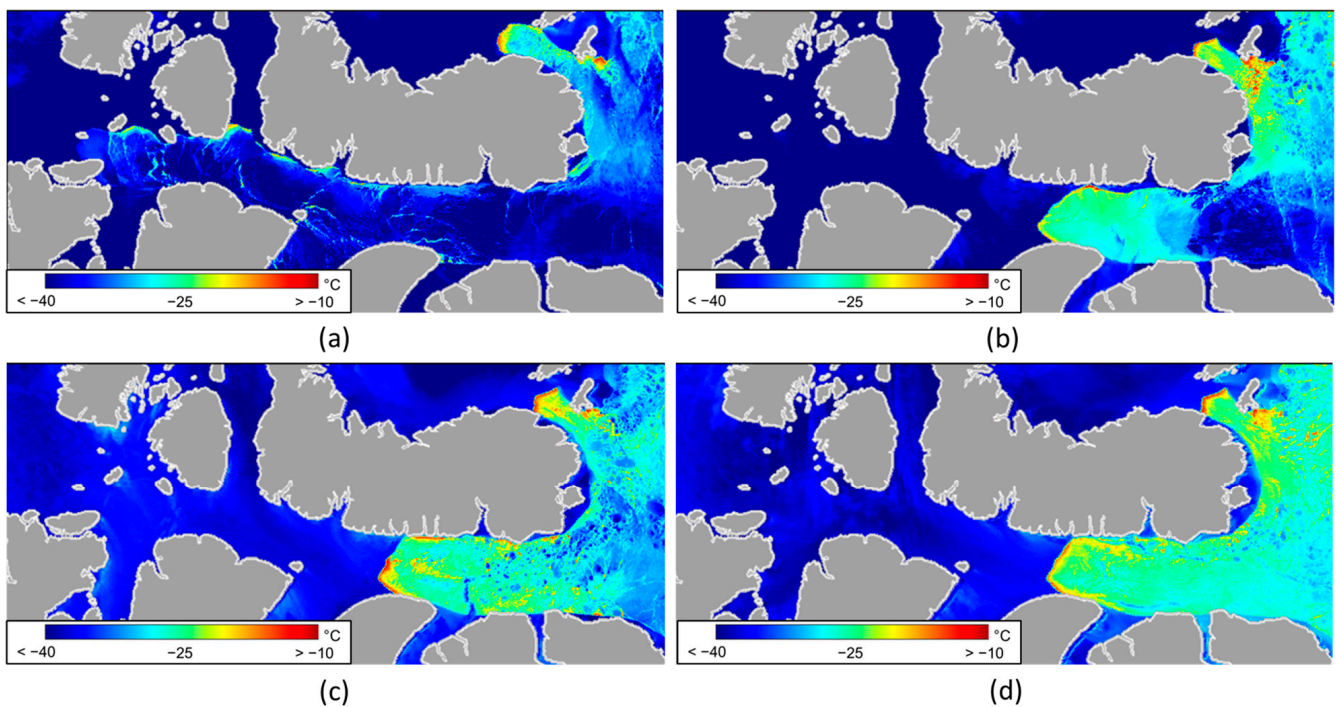


Figure 9. CASSTA mapping with land mask for 2019, including (a) 14 January, (b) 17 February, (c) 24 March and (d) 14 April. Lancaster Sound appears close to freezing solid in January, but a month later the ice arch is established and provides an excellent thermal contrast to the solid ice to the west. Once the ice arch forms, the surface temperatures are significantly warmer in the polynya than the surrounding ice pack.

4. Discussion

4.1. Location and Duration of Ice Arch

The results establish a high interannual variability of the location and duration of the Lancaster Sound ice arch. Since the ice freezes eastward from Barrow Strait, it is expected that ice arches that form further west would consolidate earlier in the year. Placing the distance of the ice arch from Bylot Island in ascending order shows a negligible correlation for both the formation (-0.07) and collapse (-0.11) of the ice arch, while linear trends are insignificant (Figure 10). The ordering of distance of the ice arch from Bylot Island shows a preferred location for the structure in the vicinity of eastern Somerset Island, which is also the beginning of Barrow Strait. Despite the overall variability of the ice arch location, the seasonal position has fallen between 280 and 320 km from Bylot Island 15 times since

1979, with some consecutive years apparent in the record (1980, 1981, 1990, 1991, 1992, 1995, 1997, 2000, 2005, 2006, 2008, 2014, 2016, 2017, 2020).

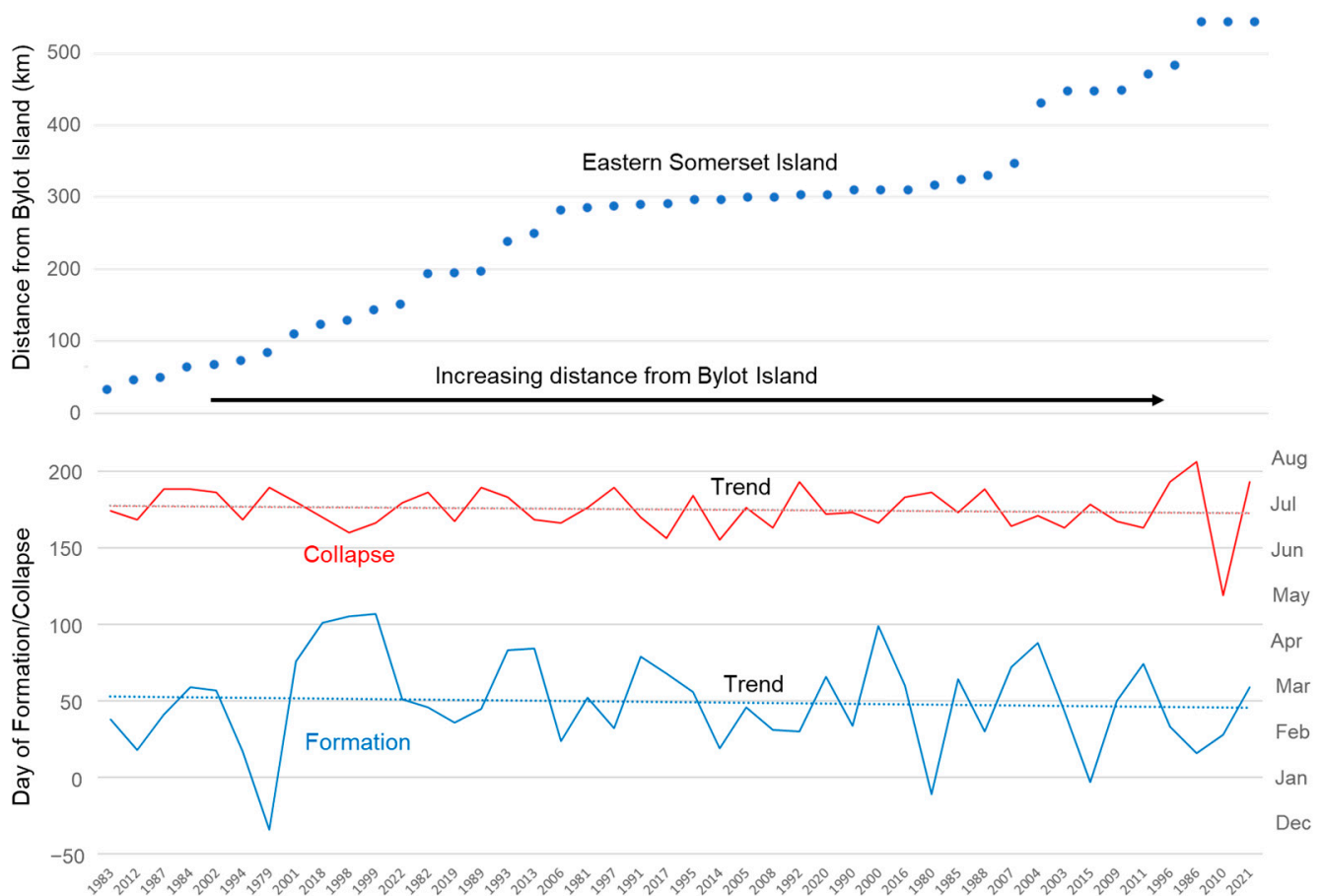


Figure 10. Distance of the Lancaster Sound ice arch from Bylot Island (top of graph) in ascending order is compared to ice arch formation and collapse (bottom of graph). Correlation and linear trends are insignificant, implying that the location of the ice arch has no effect on the timing and duration of the structure.

4.2. Thermal Signature and Ice Concentration

CASSTA mappings of the Lancaster Sound polynya during the colder months showed surface temperatures well below the freezing point of seawater, but significantly higher than the surrounding ice pack. This suggests that small leads less than the spatial resolution of the AVHRR sensor are contributing heat to the imaged pixel. Since the surface temperature of ice and snow will approximate the surface air temperature [28], then the surface of the polynya can be approximated with a binary solution where open water is $-1.8\text{ }^{\circ}\text{C}$ and the ice approximates the surface air temperature. Higher concentrations of ice in the polynya are, therefore, associated with colder surface temperatures. The surface temperature in the Lancaster Sound polynya varied considerably depending on the year and month and appeared related to ice conditions in northwestern Baffin Bay (Figure 11). This implies that the ice concentration in Lancaster Sound is influenced by the southward flow of ice from Jones Sound and the NOW.

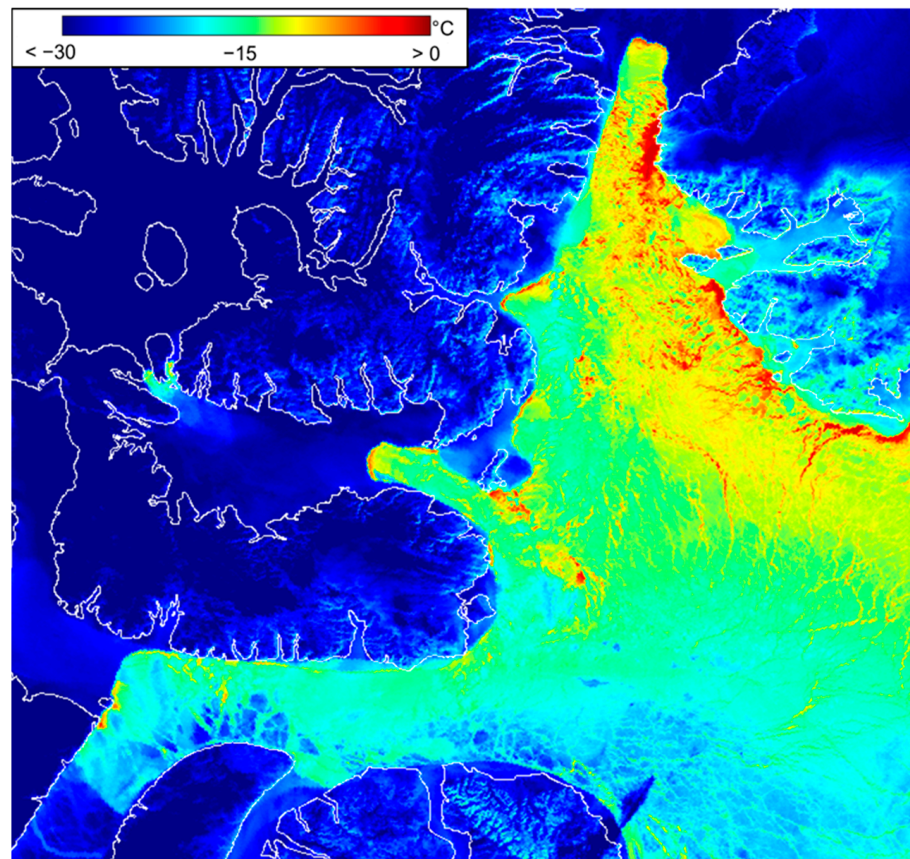


Figure 11. CASSTA mapping of the NOW, Jones Sound and Lancaster Sound polynyas with coastlines outlined for 4 Apr 2016. Surface temperatures in Lancaster Sound are well below the freezing point of seawater, implying that the increased temperature is the result of thermal contribution to the pixel by sub-resolution leads. Warmer temperatures are indicative of reduced ice cover, but there are no large regions of open water. This was typical of Lancaster Sound during the colder months. The image also shows that the eastward outflow of ice from the Lancaster Sound polynya is influenced by ice conditions in northwestern Baffin Bay owing to the southward moving floes from the NOW and Jones Sound.

4.3. Influence of Arctic Amplification and Comparison to the NOW

Arctic amplification is the observation that surface air temperatures are rising more rapidly than anywhere else in the world [29,30], which has led to the significant loss of multiyear ice in the Arctic basin [31]. The trend toward first year ice that is thinner and more easily melted is a factor in the changing Arctic icescape [32]. The overall statistics of ice arch formation for Lancaster Sound imply that polar warming is leading to a reduction in ice arch duration, but the data tell a different story when divided evenly from 1979 to 2000 and from 2001 to 2022 (Figure 12). From 1979 to 2000, the linear trend indicates that the ice arch is forming more than two months later (p -value = 0.029), while there is a weak statistical significance (p -value = 0.091) for a modest decrease in the ice arch collapse over that span. From 2001 to 2022, there is essentially no trend in either the ice arch formation or collapse. Data from this study indicate that the reduction in ice arch duration is a result of earlier collapse dates over the entire study period and later formation dates, particularly from 1979 to 2000. Arctic warming has accelerated since 2000 [33], suggesting that a complex system of factors beyond increasing surface air temperatures are involved in the ice arch formation, which can be extended to the annual dynamics of the Lancaster Sound ice arch in general.

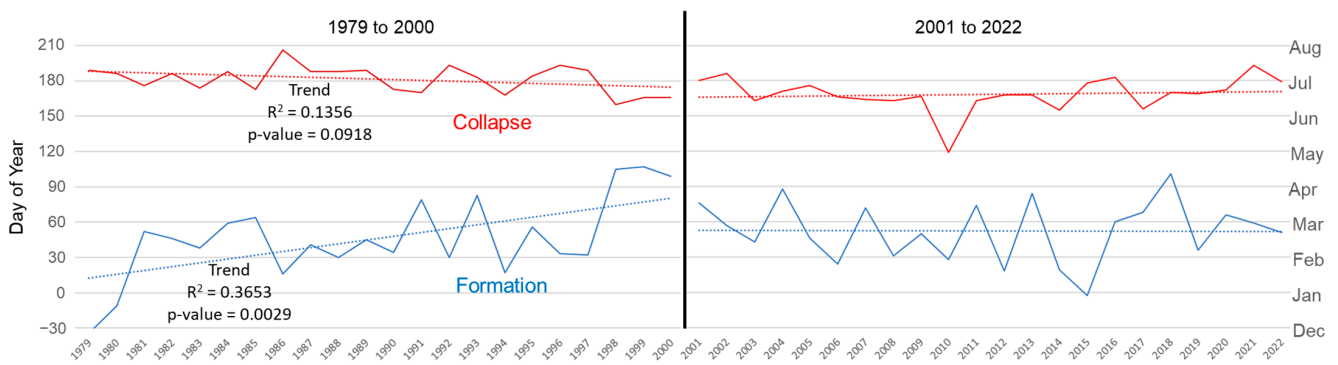


Figure 12. Trends for the formation and collapse of the Lancaster Sound ice arch for 1979 to 2000 (left side of graph) and from 2001 to 2022 (right side of graph). Formation date increases dramatically from 1979 to 2000, with a small decrease in collapse date. From 2001 to 2022, there is essentially no trend in either the date of formation or collapse.

A similar study of the NOW ice arch, approximately 600 km north of Lancaster Sound, was carried out for 1979 to 2019 [34]. The NOW is the largest recurring polynya in the Canadian Arctic [35] and, similar to Lancaster Sound, demonstrates a high variability in ice arch duration from season to season. Although variable interannually, the NOW ice arch average formation and collapse dates are 11 January and 28 June, respectively, compared to 18 February and 23 June for the Lancaster Sound ice arch, resulting in a longer average ice arch duration for the NOW. The NOW dataset was extended to 2022 for this study to allow a direct comparison with the Lancaster Sound polynya to determine if a relationship exists between interannual fluctuations of ice arch duration (Figure 13). From 1979 to 2022, the NOW showed a reduction of 85 days of ice arch duration compared to 48 days for Lancaster Sound. The datasets reveal a weak correlation (0.30); however, the correlation increases slightly (0.31) from 1979 to 2000 and becomes negligible (0.18) from 2001 to 2022. This suggests that large scale atmospheric effects in the eastern Canadian Arctic have limited universal influence on the ice arch formation for the NOW and Lancaster Sound polynya, especially since 2000.

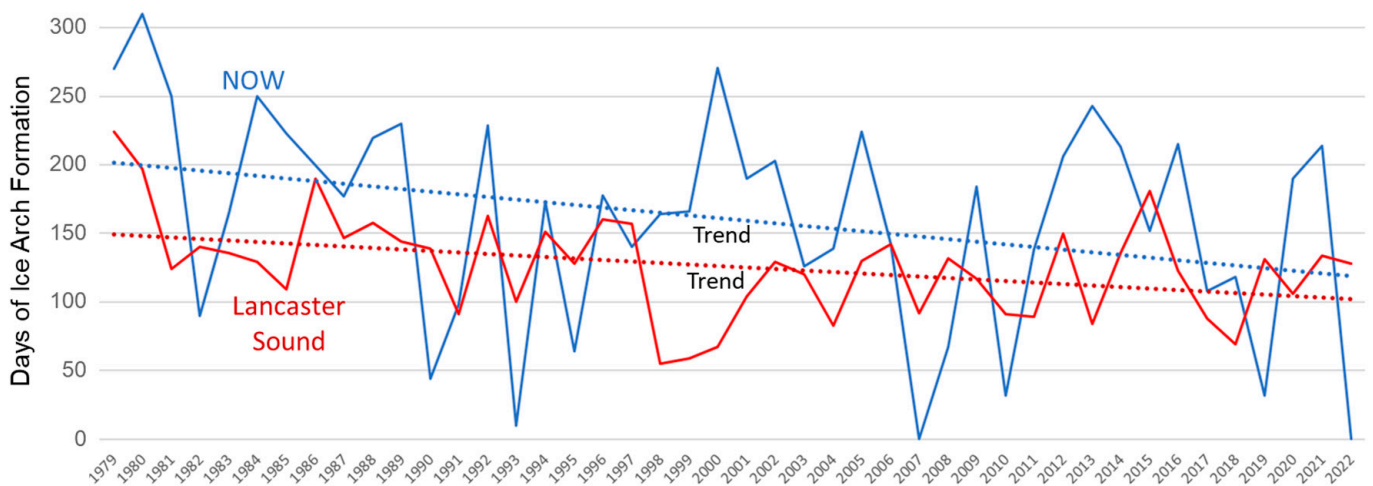


Figure 13. Days of ice arch formation and linear trends for the NOW (blue) and the Lancaster Sound polynya (red) from 1979 to 2022. Both datasets are highly variable, with an overall downward trend of ice arch duration since 1979. Some peaks and valleys in the graphs align, but overall, there is only a weak positive correlation from 1979 to 2000 and negligible correlation from 2000 to 2022.

5. Conclusions

Lancaster Sound is an important region of the Arctic from an ecological and cultural standpoint. The area is also critical from a strategic and economic perspective since it represents the eastern entrance of the Northwest Passage. Regional trends in ice dynamics are an important area of study for this environmentally sensitive area. An analysis of satellite imagery dating back to 1979 shows that a polynya has formed every year during the colder months. The Lancaster Sound polynya is characterized by an ice arch that demarcates its western border. The ice arch generally forms in mid-February and collapses in late June. The following is a summary of the major findings of the study.

- The ice arch location demonstrates a high interannual variability with 512 km between the eastern and western extremes. Historically, the ice arch occurs at various locations along Lancaster Sound and Barrow Strait, but it has consolidated in the vicinity of eastern Somerset Island 15 times in the satellite record. The overall trend is for a westward movement of the ice arch of 115 km, which is statistically weak.
- Since Barrow Strait and Lancaster Sound generally freeze eastward until the ice arch forms, it is expected that ice arches further to the west should consolidate earlier; however, the data indicates that the ice arch location has no bearing on either the formation or collapse of the structure.
- Although highly variable, a linear trend from 1979 to 2022 shows a reduction of 48 days in ice arch duration. The shorter ice duration is attributable to earlier collapse dates over the entire span of the study and later formation dates, particularly from 1979 to 2000. The latter seems counterintuitive given the acceleration of Arctic amplification in the region since 2000.

This study has uncovered interesting aspects of the Lancaster Sound polynya that will aid scientists working on oceanographic, biological and underwater acoustic investigations in the region. The satellite data have revealed what is arguably the most variable recurring polynya in the Canadian Arctic, with underlying physical properties that require further research.

Funding: The article process charge was funded by the Canadian Defence Academy Research Program.

Data Availability Statement: Satellite Advanced Very High Resolution (AVHRR) data is available on-line at the National Oceanic and Atmospheric Administration (NOAA) Comprehensive Large Array-data Stewardship System (CLASS).

Conflicts of Interest: The author declares no conflict of interest.

References

1. Yao, T.; Tang, C.L. The formation and maintenance of the North Water Polynya. *Atmos.-Ocean* **2003**, *41*, 187–201. [CrossRef]
2. Steffen, K. Warm Water Cells in the North Water, Northern Baffin Bay During Winter. *J. Geophys. Res.* **1985**, *90*, 9129–9136. [CrossRef]
3. Darby, M.S.; Willmott, A.J.; Mysak, L.A. A Nonlinear Steady-State Model of the North Water Polynya, Baffin Bay. *J. Phys. Oceanogr.* **1994**, *24*, 1011–1020. [CrossRef]
4. Mysak, L.A.; Huang, F. A Latent-and Sensible-Heat Polynya Model for the North Water, Northern Baffin Bay. *J. Phys. Oceanogr.* **1992**, *22*, 596–608. [CrossRef]
5. Vincent, R.; Marsden, R. A Study of Tidal Influences in the North Water Polynya using Short Time Span Satellite Imagery. *Arctic* **2009**, *61*, 373–380. Available online: <https://www.jstor.org/stable/40513224> (accessed on 27 December 2022). [CrossRef]
6. Vincent, R.F. An Examination of the Non-Formation of the North Water Polynya Ice Arch. *Remote Sens.* **2020**, *12*, 2712. [CrossRef]
7. Hannah, C.G.; Dupont, F.; Dunphy, M. Polynyas and Tidal Currents in the Canadian Arctic Archipelago. *Arctic* **2009**, *62*, 83–95. Available online: <https://www.jstor.org/stable/40513267> (accessed on 27 December 2022). [CrossRef]
8. Smith, S.D.; Muench, R.D.; Pease, C.H. Polynyas and leads: An overview of physical processes and environment. *J. Geophys. Res.* **1995**, *95*, 9461–9479. [CrossRef]
9. Kalenitchenko, D.; Joli, N.; Potvin, M.; Tremblay, J.; Lovejoy, C. Biodiversity and Species Change in the Arctic Ocean: A View Through the Lens of Nares Strait. *Front. Mar. Sci.* **2019**, *6*, 479. [CrossRef]
10. Karnovsky, N.J.; Hunt, G.L. Estimation of carbon flux to dovekeys (Alle alle) in the North Water. *Deep Sea Res. Part II Top. Stud. Oceanogr.* **2002**, *49*, 5117–5130. [CrossRef]
11. Marchese, C. Biodiversity hotspots: A shortcut for a more complicated concept. *Glob. Ecol. Conserv.* **2015**, *3*, 297–309. [CrossRef]

12. Leblond, P.H. On the surface circulation in some channels of the Canadian Arctic Archipelago. *Arctic* **1980**, *33*, 189–197. Available online: <https://www.jstor.org/stable/40509282> (accessed on 31 January 2023). [[CrossRef](#)]
13. Government of Canada: Tides, Currents, and Water Levels. Available online: <https://tides.gc.ca/en> (accessed on 27 December 2022).
14. Prinsenberg, S.J.; Hamilton, J. Monitoring the volume, freshwater and heat fluxes passing through Lancaster sound in the Canadian arctic archipelago. *Atmos.-Ocean* **2005**, *43*, 1–22. [[CrossRef](#)]
15. Fissel, D.B.; Lemon, D.D.; Knight, D.N. An oceanographic survey of the Canadian Arctic Archipelago, March 1983. In *Canadian Contract Report of Hydrography and Ocean Sciences*; Fisheries and Oceans Canada: Ottawa, ON, Canada, 1984; p. 355.
16. Welch, H.E.; Bergmann, M.A.; Siferd, T.D.; Martin, K.A.; Curtis, M.F.; Crawford, R.E.; Conover, R.J.; Hop, H. Energy flow through the marine ecosystem of the Lancaster Sound region, Arctic Canada. *Arctic* **1992**, *45*, 343–357. Available online: <https://www.jstor.org/stable/40511483> (accessed on 27 December 2022). [[CrossRef](#)]
17. Pieńkowski, A.J.; England, J.H.; Furze, M.F.A.; MacLean, B.; Blasco, S. The late Quaternary environmental evolution of marine Arctic Canada: Barrow Strait to Lancaster Sound. *Quat. Sci. Rev.* **2014**, *91*, 184–203. [[CrossRef](#)]
18. Halliday, W.D.; Dawson, J.; Yurkowski, D.J.; Doniol-Valcroze, T.; Ferguson, S.H.; Gjerdrum, C.; Hussey, N.E.; Kochanowicz, Z.; Mallory, M.L.; Marcoux, M.; et al. Vessel risks to marine wildlife in the Tallurutiup Imanga National Marine Conservation Area and the eastern entrance to the Northwest Passage. *Environ. Sci. Policy* **2022**, *127*, 181–195. [[CrossRef](#)]
19. Hibler, W.; Hutchings, J.; Ip, C. Sea-ice arching and multiple flow States of Arctic pack ice. *Ann. Glaciol.* **2006**, *44*, 339–344. [[CrossRef](#)]
20. Lyu, H.; Huang, W.; Mahdianpari, M. A Meta-Analysis of Sea Ice Monitoring Using Spaceborne Polarimetric SAR: Advances in the Last Decade. *IEEE J. Sel. Top. Appl. Earth Obs. Remote Sens.* **2022**, *15*, 6158–6179. [[CrossRef](#)]
21. Preußner, A.; Heinemann, G.; Schefczyk, L.; Willmes, S. A Model-Based Temperature Adjustment Scheme for Wintertime Sea-Ice Production Retrievals from MODIS. *Remote Sens.* **2022**, *14*, 2036. [[CrossRef](#)]
22. Preußner, A.; Ohshima, K.I.; Iwamoto, K.; Willmes, S.; Heinemann, G. Retrieval of Wintertime sea ice Production in Arctic Polynyas Using Thermal Infrared and Passive Microwave Remote Sensing Data. *J. Geophys. Res. Ocean.* **2019**, *124*, 5503–5528. [[CrossRef](#)]
23. Shen, X.; Zhang, J.; Zhang, X.; Meng, J.; Ke, C. Sea Ice Classification Using Cryosat-2 Altimeter Data by Optimal Classifier-Feature Assembly. *IEEE Geosci. Remote Sens. Lett.* **2017**, *14*, 1948–1952. [[CrossRef](#)]
24. NOAA’s Comprehensive Large Array-Data Stewardship System. Available online: <https://www.bou.class.noaa.gov/saa/products/welcome> (accessed on 17 December 2022).
25. Herman, G.; Goody, R. Formation and Persistence of Summertime Arctic Stratus Clouds. *J. Atmos. Sci.* **1976**, *33*, 1537–1553. [[CrossRef](#)]
26. Vincent, R. The Case for a Single Channel Composite Arctic Sea Surface Temperature Algorithm. *Remote Sens.* **2019**, *11*, 2393. [[CrossRef](#)]
27. Vincent, R.F.; Marsden, R.F.; Minnett, P.J.; Buckley, J.R. Arctic waters and marginal ice zones: 2. An investigation of arctic atmospheric infrared absorption for advanced very high resolution radiometer sea surface temperature estimates. *J. Geophys. Res.* **2008**, *113*, C08044. [[CrossRef](#)]
28. Nielsen-Englyst, P.; Høyer, J.L.; Madsen, K.S.; Tonboe, R.; Dybkjær, G.; Alerskans, E. In Situ Observed Relationships between Snow and Ice Surface Skin Temperatures and 2 m Air Temperatures in the Arctic. *Cryosphere* **2019**, *13*, 1005–1024. [[CrossRef](#)]
29. Serreze, M.C.; Francis, J.A. The Arctic Amplification Debate. *Clim. Chang.* **2006**, *76*, 241–264. [[CrossRef](#)]
30. Cohen, J.; Screen, J.A.; Furtado, J.C.; Barlow, M.; Whittleston, D.; Coumou, D.; Francis, J.; Dethloff, K.; Entekhabi, D.; Overland, J.; et al. Recent Arctic amplification and extreme mid-latitude weather. *Nat. Geosci.* **2014**, *7*, 627–637. [[CrossRef](#)]
31. Kwok, R. Arctic sea ice thickness, volume, and multiyear ice coverage: Losses and coupled variability (1958–2018). *Environ. Res. Lett.* **2018**, *13*, 105005. [[CrossRef](#)]
32. Korosov, A.A.; Rampal, P.; Pedersen, L.T.; Saldo, R.; Ye, Y.; Heygster, G.; Lavergne, T.; Aaboe, S.; Girard-Ardhuin, F. A new tracking algorithm for sea ice age distribution estimation. *Cryosphere* **2018**, *12*, 2073–2085. [[CrossRef](#)]
33. Ballinger, T.J.; Overland, J.E.; Wang, M.; Bhatt, U.S.; Brettschneider, B.; Hanna, E.; Hanssen-Bauer, I.; Kim, S.-J.; Thoman, R.L.; Walsh, J.E. *Surface Air Temperature*; NOAA Technical Report OAR ARC; 21-02; National Oceanic and Atmospheric Administration: Washington, DC, USA, 2021. [[CrossRef](#)]
34. Vincent, R.F. A Study of the North Water Polynya Ice Arch using Four Decades of Satellite Data. *Sci. Rep.* **2019**, *9*, 20278. [[CrossRef](#)]
35. Tremblay, J.-É.; Gratton, Y.; Carmack, E.C.; Payne, C.D.; Price, N.M. Impact of the large-scale Arctic circulation and the North Water Polynya on nutrient inventories in Baffin Bay. *J. Geophys. Res.* **2002**, *107*, 26-1–26-14. [[CrossRef](#)]

Disclaimer/Publisher’s Note: The statements, opinions and data contained in all publications are solely those of the individual author(s) and contributor(s) and not of MDPI and/or the editor(s). MDPI and/or the editor(s) disclaim responsibility for any injury to people or property resulting from any ideas, methods, instructions or products referred to in the content.